



Highly selective and ultrasensitive detection of nitrite based on fluorescent gold nanoclusters

Hongying Liu^a, Guohai Yang^a, E.S. Abdel-Halim^b, Jun-Jie Zhu^{a,*}

^a State Key Laboratory of Analytical Chemistry for Life Science, School of Chemistry and Chemical Engineering, Nanjing University, Nanjing 210093, PR China

^b Petrochemical Research Chair, Chemistry Department, College of Science, King Saud University, PO Box 2455, Riyadh 11451, Kingdom of Saudi Arabia, Saudi Arabia

ARTICLE INFO

Article history:

Received 14 August 2012

Received in revised form

28 October 2012

Accepted 8 November 2012

Available online 27 November 2012

Keywords:

Gold nanoclusters

Nitrite

Optical sensors

Detection

Water analysis

ABSTRACT

Near-infrared fluorescent gold nanoclusters (AuNCs) were prepared by sonochemical method and applied for the selective and sensitive detection of nitrite. The fluorescence of AuNCs could be selectively quenched by nitrite, and the mechanism was discussed in detail. The fluorescence intensity decreased linearly upon the increasing concentration of nitrite in a wide range of 2.0×10^{-8} M to 5.0×10^{-5} M. The detection limit was only 1.0 nM ($S/N=3$), which was much lower than the maximum admissible concentration of 2.2 μ M required by the European Community. The proposed method was also applied for the determination of nitrite in real water samples. The present method exhibited excellent analytical performances, such as wide detection range, good selectivity, high sensitivity, and the applicability in neutral medium.

© 2012 Elsevier B.V. All rights reserved.

1. Introduction

Nitrite, as preservatives and fertilizing agents for food, widely exist in the environments. The increasing concentration of nitrite in real water has caused serious hazards to public health and environments [1–3]. It is reported that nitrite can damage the nervous system, spleen and kidneys, and have a strong correlation with high cancer levels when its concentration is higher than 4.5 mg mL^{-1} [4]. Therefore, it is very important to quantitatively detect nitrite in drinking water sources, waste water treatment, and food industry. Some methods such as chemiluminescence (CL) [5–7], titrimetric [8], chromatographic [9,10], capillary electrophoresis [11,12], and electrochemical methods [13–15] have been developed for the analysis of nitrite. However, some methods are unsuitable for the routine ultra-trace determination. For instance, spectrophotometric methods suffer from poor sensitivity and interference from other anions. Although chromatographic methods possess high sensitivity and selectivity, they are often time-consuming. Capillary electrophoresis has a complicated process and requires relatively expensive instruments. Compared with these methods, fluorescence method has attracted much attention with the advantage of low cost, simplicity, speed, high sensitivity, and low limit of detection [16,17].

Thus, it is highly desirable to develop sensitive and selective fluorescent sensors for the detection of nitrite.

Highly efficient and stable fluorescent probes are of great importance to fluorescence-based nitrite sensors. Intensive efforts have been focused on the exploration of new efficient fluorescent materials [18,19]. A variety of organic fluorophores have been successfully applied to detect nitrite [20,21]. Unfortunately, the performances of these sensors are limited by their poor sensitivity and stability [22,23]. Quantum dots with multifarious advantages over organic dyes such as excellent fluorescence properties, higher photochemical stability and excellent resistant to chemical degradation have attracted great attention and achieved encouraging developments in the analytical application [24,25]. Thus, QDs-based fluorescent sensors have great potential to overcome the problems encountered by organic fluorophore-based sensors. However, the inherent compositional toxicity limits their applications [26,27]. In addition, fluorescent probes emitting in the near-infrared window between 650 nm and 900 nm, have been extensively studied in some active field, benefiting from their attractive advantages such as improved tissue penetration, lower background interference, and reduced photochemical damage [28,29]. Thus, further explorations on novel fluorescent nitrite sensors in the near-infrared region are of great importance. Recently, gold nanoclusters (AuNCs), an attractive fluorescent probe [30–33], are of particular interest because of its low toxicity, excellent biocompatibility and stability, good solubility, and excellent luminescence properties [34]. AuNCs has been employed in some research fields, such as biological imaging [35,36], ions sensing [37–39], and

* Corresponding author. Tel./fax: +86 25 83597204.

E-mail addresses: jjzhu@mail.nju.edu.cn, jjzhu@nju.edu.cn (J.-J. Zhu).

biosensors [40,41]. To the best of our knowledge, the optical sensor for the detection of nitrite using AuNCs as the fluorescent probe has not been reported.

In our previous report, highly fluorescent and water-soluble AuNCs with near-infrared-emission were prepared via a facile and rapid sonochemical method under mild conditions [42]. The obtained bovine serum albumin-stabilized AuNCs (BSA–AuNCs) possess strong fluorescence signal, large Stokes shifts, good photostability, and stimuli-responsive properties. All of these properties showed that AuNCs could be used as promising fluorescent probe candidates for optical sensor. In this work, BSA–AuNCs are used to construct nitrite sensor for the first time. The fluorescence of BSA–AuNCs was gradually decreased with the increase of nitrite concentrations, and the corresponding limit of detection was 1 nM. The fluorescence quenching mechanism of BSA–AuNCs was also discussed. Moreover, the sensor was successfully applied to natural water samples with precise and accurate results. The proposed sensor exhibited advantages of high selectivity, wide detection range, and low limit of detection, revealing the potential application of BSA–AuNCs in sensors.

2. Experimental

2.1. Reagents

BSA was purchased from Sigma-Aldrich. Chloroauric acid (HAuCl₄) was obtained from Shanghai Reagent Co. (Shanghai, China). All other reagents were of analytical reagent grade and used without further purification. Aqueous solutions were prepared with doubly distilled water at room temperature.

2.2. Apparatus

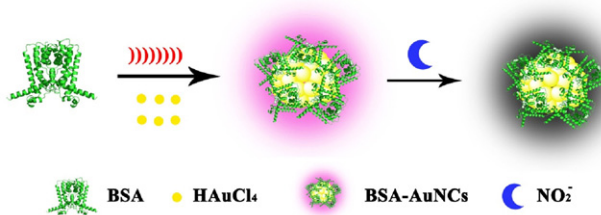
The UV–Visible absorption spectra were carried out on a Shimadzu 3600 UV–Visible spectrometer (Shimadzu, Japan). The fluorescence measurements were carried out on Edinburgh FLS920P fluorescence spectrometer (Edinburgh Instruments Ltd., UK). The high resolution transmission electron microscopy (HRTEM) images were observed by JEOL JEM-2100. X-ray photoelectron spectroscopy (XPS) was carried out on an ESCALAB MK II X-ray photoelectron spectrometer. Fourier transform infrared (FTIR) spectroscopic measurements were performed on a Bruker model VECTOR22 fourier transform spectrometer using KBr pressed disks.

2.3. Synthesis of BSA–AuNCs

The synthesis of BSA–AuNCs was performed according to the literature [42]. Briefly, HAuCl₄ solution (20 mL, 10 mM) was added into the BSA solution (20 mL, 50 mg mL⁻¹) under vigorous stirring. After reaction for 2 min, pH value was adjusted to 12 by the addition of NaOH solution (2 mL, 1 M). Then the mixture was exposed to high intensity ultrasonic irradiation (Xinzhì Co., China, JY92-2D, 10 mm diameter; Ti-horn, 20 kHz, 60 W cm⁻²) under ambient air for a certain time. After the reaction, light brown solutions were obtained. The procedure for the synthesis of BSA–AuNCs and the fabrication of nitrite sensor were shown in Scheme 1. First, fluorescent BSA–AuNCs were obtained by one-step sonochemical method. Then the fluorescence of BSA–AuNCs was quenched dramatically in the presence of nitrite.

2.4. Fluorescence detection

Nitrite aqueous solutions with different concentrations were freshly prepared. For quenching studies, AuNCs and NaNO₂ with



Scheme 1. Scheme of the synthetic strategy for BSA–AuNCs and the principle of nitrite sensing.

different concentrations were mixed in 50 mM phosphate buffer solutions (PBS, pH=7.4), and then equilibrated for 20 min. The fluorescence spectra were measured at 670 nm with the excitation wavelength at 350 nm.

2.5. Selectivity measurements

The following inorganic salts were used for selectivity experiments: sodium acetate, sodium chloride, sodium nitrite, sodium nitrate, sodium carbonate, and so on. 5 mM salt stock solution was prepared by ultrapure water. Subsequently, the salt solution was prepared by serial dilution with PBS (50 mM, pH=7.4), and then mixed with BSA–AuNCs solution in the absence and presence of NaNO₂.

2.6. Physical characterization of the fluorescence quenching

To get the HRTEM images of NO₂⁻-treated BSA–AuNCs, 5 μL of 1 mM NaNO₂ was added to 1 mL of 40 nM BSA–AuNCs solution. After incubation for 20 min, the suspensions were deposited onto copper grids with carbon support by slowly evaporating the solvent in air at room temperature.

3. Results and discussion

3.1. Characterization of the as-prepared BSA–AuNCs

The BSA–AuNCs were synthesized via sonochemical method and characterized by fluorescence spectra, photograph, HRTEM, FTIR and XPS, as shown in Fig. 1. The obtained BSA–AuNCs showed a deep brown color under visible light and emitted bright-red fluorescence under UV light. They exhibited a broad absorption at 500 nm and a strong emission peak at 670 nm (Fig. 1A). Compared with the phase solution method, a red shift of the emission wavelength from 620 nm to 670 nm for BSA–AuNCs was observed by sonochemical method. It suggested that the obtained BSA–AuNCs have higher potential in biosensor due to the low tissue absorption and scattering effects in the near-infrared region. Moreover, the as-prepared BSA–AuNCs showed stronger fluorescence than that by the phase solution method, which was consistent with our previous report [42]. The reasons may be as follows: when liquids are irradiated with ultrasonic irradiation, acoustic cavitation produces high temperature (5000 K), high pressures (20 MPa) and cooling rates (107 K/s), which can provide a platform for the growth of materials with an abundance of energy and extremely fast kinetics, thus promoting chemical reactions [43]. These results suggested the as-prepared BSA–AuNCs herein were favorable for bioapplications. Furthermore, the morphology of the BSA–AuNCs was characterized by HRTEM. As demonstrated in Fig. 1B, the obtained BSA–AuNCs were 1.8 nm in diameter with narrow size distribution. In addition, XPS was employed to investigate the oxidation states of the BSA–AuNCs. The Au 4f_{7/2} spectrum could be deconvoluted into

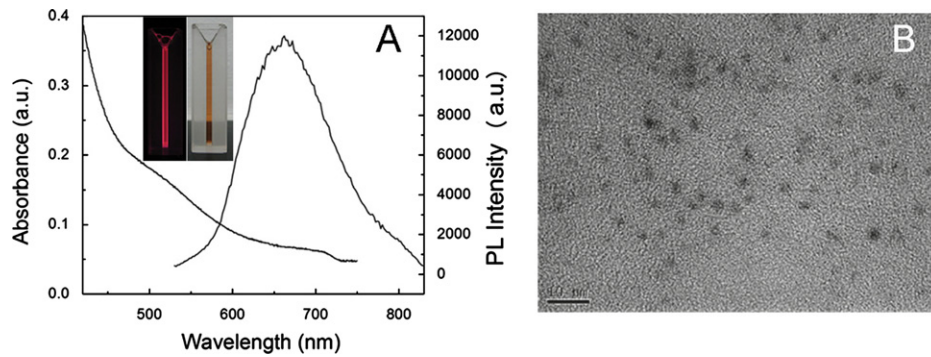


Fig. 1. (A) Fluorescence emission and UV-Visible absorption spectra of the BSA-AuNCs solution. Inset: photographs under ultraviolet light (left) and visible light (right) of the BSA-AuNCs solution. (B) HRTEM images of BSA-AuNCs.

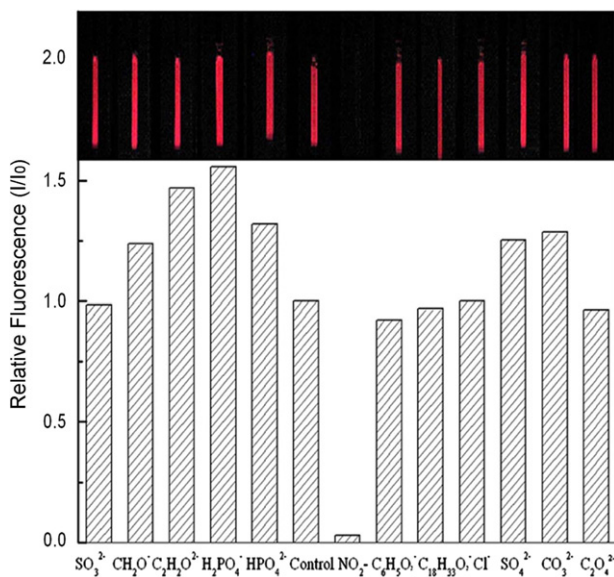


Fig. 2. Relative fluorescence (I/I_0) of BSA-AuNCs solution in the presence of 50 μM various anions. Inset: Photographs of BSA-AuNCs solution in the presence of 50 μM various anion under UV light.

two peaks at 84.0 eV and 85.1 eV, which were assigned to the binding energies of elemental Au (0) and cationic Au (+1), respectively. Finally, FTIR was used to confirm the successful binding between BSA and AuNCs.

3.2. Selective fluorescence quenching by nitrite

As shown in Fig. 2, the fluorescence of BSA-AuNCs at 670 nm was almost completely quenched (97%) upon the addition of nitrite, which strongly proved that nitrite was an effective quencher to BSA-AuNCs fluorescence. To further prove the quenching effect by nitrite, the fluorescence response was measured in the presence of common anions, including SO_3^{2-} , CH_2O^- , $\text{C}_2\text{H}_2\text{O}_2^-$, H_2PO_4^- , HPO_4^{2-} , $\text{C}_6\text{H}_5\text{O}^-$, SO_4^{2-} , $\text{C}_{18}\text{H}_{33}\text{O}^-$, Cl^- , $\text{C}_2\text{O}_4^{2-}$ and CO_3^{2-} . As shown in Fig. 2, only nitrite could induce a drastic decrease in the fluorescence intensity while no obvious fluorescence changes were observed in the presence of other anions. Under UV light, the similar results were also observed (Fig. 2 inset). The above results indicated that the proposed sensor had high selectivity towards nitrite.

3.3. Mechanism of the quenching effect

As shown in Fig. 2, the BSA-AuNCs solution exhibited bright-red fluorescence under 365 nm UV light. After addition of nitrite,

weak fluorescence was observed (Fig. 2). The corresponding emission spectrum was also investigated. The results showed that the fluorescence wavelength remained unchanged while the fluorescence intensity decreased with the addition of nitrite. The fluorescence quenching effect may come from the BSA-AuNCs aggregation. The HRTEM images of BSA-AuNCs in the absence and presence of nitrite were used to confirm the proposed mechanism. As shown in Fig. 3A, no aggregation appeared in the absence of the nitrite. After addition of nitrite, the BSA-AuNCs aggregated and eventually led to appearance of precipitate (Fig. 3B). The results indicated that the quenching of BSA-AuNCs fluorescence was caused by the aggregation of AuNCs, which was induced by the NO_2^-/BSA interaction. The obtained results were consistent with previous reports [30,44].

3.4. Optimization of experimental conditions

Prior to the fluorescence detection, some factors including pH value, reaction time, and concentration of BSA-AuNCs were optimized.

3.4.1. pH selection

To improve the efficiency of the proposed sensor, the relationship between the fluorescence intensity of BSA-AuNCs and pH value was studied at first. The result showed that pH value did not affect the fluorescence intensity obviously. Then, the relationship between the fluorescence intensity of BSA-AuNCs in the presence of nitrite and pH value was also investigated. The fluorescence intensity of BSA-AuNCs in the presence of nitrite decreased most effectively at pH value was 7.4. Therefore, pH 7.4 was selected in the following experiments.

3.4.2. Time selection

A time-dependent fluorescence intensity change was monitored upon addition of nitrite, as shown in Fig. 4. The fluorescence intensity at 670 nm was quenched by 80% within 5 min, and the value was up to 95% for 20 min, indicating that the reaction was completed within 20 min. Therefore, 20 min was selected as the reaction time.

3.4.3. The concentration of BSA-AuNCs

Generally, lower concentration of fluorescent probe has better sensitivity, while higher concentration has broader detection range. Therefore, the influence of the concentration of BSA-AuNCs on the efficiency of fluorescence quenching was studied. The high efficiency was observed at low BSA-AuNCs concentration in the presence of the same concentration of nitrite, and this suggested that low limit of detection could be reached. However, a broader detection range was observed at higher concentration

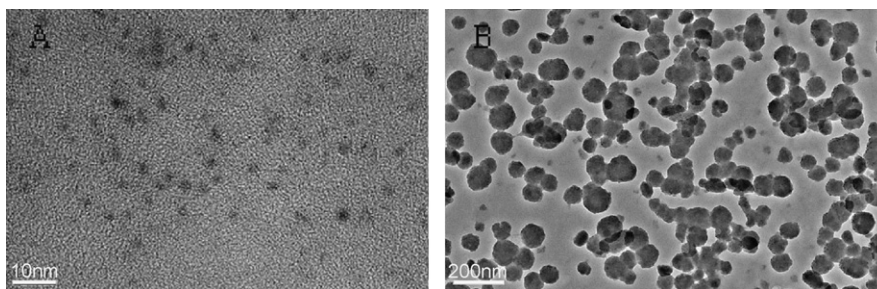


Fig. 3. The HRTEM images of the BSA-AuNCs (A), and the BSA-AuNCs in the presence of 5 μM nitrite (B).

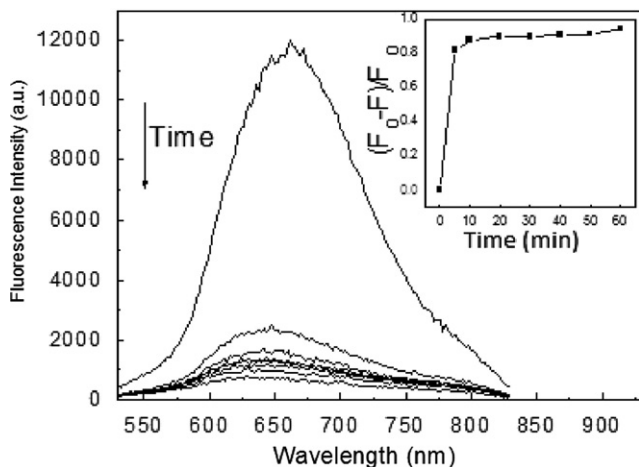


Fig. 4. Time-dependent fluorescence intensity of the BSA-AuNCs to nitrite. The inset shows $(F_0 - F)/F_0$ plotted against time in the presence of nitrite, where F_0 and F are the fluorescence intensity of the BSA-AuNCs at 670 nm in the absence and presence of nitrite, respectively.

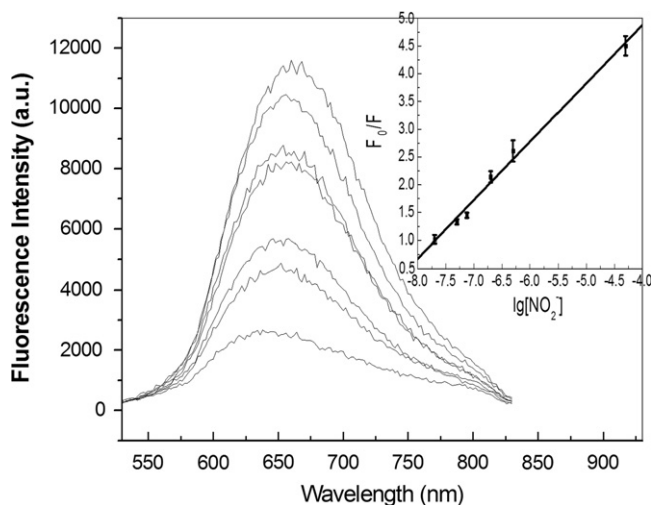


Fig. 5. Fluorescence emission spectra of BSA-AuNCs in the presence of different concentration of nitrite from 0 μM to 50 μM . Inset: Plot of the fluorescence intensity ratio of BSA-AuNCs at 670 nm versus the logarithmic of the concentration of nitrite.

of BSA-AuNCs. Considering limit of detection and detection range, the concentration of 40 nM for BSA-AuNCs was selected.

3.5. Fluorescence detection of nitrite

To evaluate the sensitivity, the fluorescence change was monitored with the addition of nitrite. As observed in Fig. 5, the fluorescence intensity of BSA-AuNCs was gradually decreased

Table 1

Comparison with the results for the determination of nitrite by other methods.

Method	Linear range ($\mu\text{g/mL}$)	Limit of detection ($\mu\text{g/mL}$)	Ref
Flow-injection	0.03–4.0	0.02	[45]
HPLC	0.000575–0.092	0.00046	[46]
FIA-Griess method	0.00046–0.027	0.009	[47]
ECL technique	1–500	0.1	[48]
Electrochemical method	0.5–100	0.1	[49]
Other optical methods	0.0004–0.2	0.0001	[50]
	0–3.22	0.028	[51]
Near-infrared optical method	0.00092–2.3	0.000046	This work

upon the increase concentration of nitrite. Furthermore, the efficiency of fluorescence quenching was analyzed by Stern-Volmer equation: $F_0/F = 1 + K_{sv} [Q]$, where F_0 and F are the fluorescence intensity of BSA-AuNCs at 670 nm in the absence and presence of nitrite, respectively. K_{sv} is the Stern-Volmer fluorescence quenching constant, which is a yardstick of the quenching efficiency of quencher, and $[Q]$ is the concentration of quencher ($[\text{NO}_2^-]$). The inset in Fig. 5 showed a Stern-Volmer plot of the fluorescence quenching of the BSA-AuNCs by nitrite, which exhibited a good linear relationship in a range of $2.0 \times 10^{-8} \text{ M}$ to $5.0 \times 10^{-5} \text{ M}$ ($R=0.9961$). K_{sv} was calculated to be $1.0509 \times 10^6 \text{ M}^{-1}$ by linear regression of the plots. The limit of detection (1.0 nM) was calculated using $3 \sigma/S$, where σ is the standard deviation of the blank signal, and S is the slope of the linear calibration plot.

A comparison of detection performance between this work and other reported methods in sensitivity and linear range was carried out. As shown in Table 1, our developed assay exhibits a lower limit of detection and a wider linear range. Moreover, the detection medium in the proposed method tended to neutral, which would greatly benefit its bio-application.

3.6. Applications

To test the feasibility, the proposed method was applied to determine the concentration of nitrite in real water samples including local groundwater, tap water, pond water, and wastewater. The samples were followed by filtration through a 0.45 μm membrane filter to eliminate the possible interference caused by the turbidity of particles, and then diluted appropriately to the concentration within the linear range of detection. The results shown in Table 2 indicated that nitrite was found in all samples and no obvious difference between the proposed method and the standard addition was observed. The recoveries of nitrite obtained by the proposed method ranged from 96.99% to 99.51% (mean $98.02 \pm 1.49\%$), matching those obtained by the standard method ($96.33\text{--}99.56\%$, mean $98.19 \pm 1.86\%$). Reproducibility was evaluated from the relative standard deviations (RSD) of eight repeated

Table 2
Determination of nitrite in real water samples by the proposed method.

Samples	Standard addition (μM)	Amount found (μM)	RSD (%) ($n=5$)	Recovered (%)
Tap water	0.0	0.35	3.8	99.51
	0.2	0.58	4.5	
	0.8	1.20	5.6	
Well water	0.0	0.32	2.6	96.99
	0.2	0.50	7.3	
	0.8	1.10	7.8	
Spring water	0.0	0.21	3.2	97.30
	0.2	0.39	5.4	
	0.8	1.05	8.3	
Distilled water	0.0	0.10	2.2	98.89
	0.2	0.28	4.9	
	0.8	0.86	5.6	

determinations of a stand solution containing 5×10^{-7} M nitrite in real samples. The obtained RSD were below 3.5%, indicating that the present sensor could be efficiently used to determine the concentration of nitrite in water and food samples with satisfactory reproducibility.

4. Conclusion

The near-infrared (NIR)-emitting BSA-capped AuNCs demonstrated selective fluorescence quenching towards nitrite, thereby a novel NIR fluorescence sensor for sensitive nitrite detection in neutral medium was proposed. The present method exhibited wide detection range, good selectivity, high sensitivity, neutral medium, and avoidance of coexisting substances interferences. Furthermore, the practical utility of the proposed sensor has been demonstrated by the detection of trace nitrite in real samples. The studies have demonstrated that the proposed method is greatly promising in practical applications.

Acknowledgements

We thank the help of Ximei Wu and Xiang Zhang, from Nanjing University. We greatly appreciate the financial support from National Natural Science Foundation of China (NSFC) (No 21020102038, 50972058), the support from 973 Program (No 2011CB933502), and Postdoctoral Science Foundation of China (No 2012M511236).

References

- [1] J. Davis, R.G. Campton, *Anal. Chim. Acta* 404 (2000) 241–247.
- [2] H. Kroupova, J. Machova, V. Piackova, J. Blahova, R. Dobsikova, L. Novotny, Z. Svobodova, *Ecotoxicol. Environ. Saf.* 71 (2008) 813–820.
- [3] P. Wang, Z.B. Mai, Z. Dai, Y.X. Li, X.Y. Zou, *Biosens. Bioelectron.* 24 (2009) 3242–3247.
- [4] S.A. Kyrtopoulos, *Cancer Surv.* 8 (1989) 423–442.
- [5] R.D. Cox, *Anal. Chem.* 52 (1980) 332–335.
- [6] J.E. Li, Q.Q. Li, C. Lu, L.X. Zhao, *Analyst* 136 (2011) 2379–2384.
- [7] Z. Lin, W. Xue, H. Chen, J.M. Lin, *Anal. Chem.* 83 (2011) 8245–8251.
- [8] D. Amin, K.Y. Saleem, W.A. Bashir, *Talanta* 29 (1982) 694–696.
- [9] C. Brons, C. Olieman, *J. Chromatogr.* 259 (1983) 79–86.
- [10] P. Niedzielski, I. Kurzyca, J. Siepak, *Anal. Chim. Acta.* 577 (2006) 220–224.
- [11] P.E. Jackson, P.R. Haddad, *Trends Anal. Chem.* 12 (1993) 231–238.
- [12] A.A. Okemgbo, H.H. Hill, W.F. Siems, S.G. Metcalf, *Anal. Chem.* 71 (1999) 2725–2731.
- [13] J. Wang, P. Diao, Q. Zhang, *Analyst* 137 (2012) 145–152.
- [14] R. Yue, Q. Lu, Y. Zhou, *Biosens. Bioelectron.* 26 (2011) 4436–4441.
- [15] S. Rajesh, A.K. Kanugula, K. Bhargava, G. Ilavazhagan, S. Kotamraju, C. Karunakaran, *Biosens. Bioelectron.* 26 (2010) 689–695.
- [16] M.J. Martínez-Tomé, R. Esquembre, R. Mallavia, C.R. Mateo, *J. Pharm. Biomed. Anal.* 51 (2010) 484–489.
- [17] L.C. Tabares, D. Kostrz, A. Elmalk, A. Andreoni, C. Dennison, T.J. Aartsma, G.W. Canters, *Chem. Eur. J.* 17 (2011) 12015–12019.
- [18] J.F. Callan, A.P. Silvaa, D.C. Magri, *Tetrahedron* 61 (2005) 8551–8588.
- [19] A.P. Demchenko, *Anal. Biochem.* 343 (2005) 1–22.
- [20] Q.H. Liu, X.L. Yan, J.C. Guo, D.H. Wang, L. Li, F.Y. Yan, L.G. Chen, *Spectrochim. Acta Part A* 73 (2009) 789–793.
- [21] A.A. Ensaifi, M. Amini, *Sens. Actuators B* 147 (2010) 61–66.
- [22] X. Zhou, J. Zhou, *Anal. Chem.* 76 (2004) 5302–5312.
- [23] L. Prodi, *New J. Chem.* 29 (2005) 20–31.
- [24] W.C. Chan, W.D. Maxwell, J.X. Gao, R.E. Bailey, M. Han, S. Nie, *Curr. Opin. Biotechnol.* 13 (2002) 40–46.
- [25] J.M. Klostranec, W.C.W. Chan, *Adv. Mater.* 18 (2006) 1953–1964.
- [26] W.B. Chen, R.H. Andrew, Z.B. Li, X.Y. Chen, *Nanoscale Res. Lett.* 2 (2007) 265–281.
- [27] R. Hardman, *Environ. Health Persp.* 114 (2006) 165–172.
- [28] J.V. Frangioni, *Curr. Opin. Chem. Biol.* 7 (2003) 626–634.
- [29] Y.S. Xia, C.Q. Zhu, *Analyst* 133 (2003) 928–932.
- [30] W.B. Chen, X.J. Tu, X.Q. Guo, *Chem. Commun.* (2009) 1736–1738.
- [31] C.T. Chen, W.J. Chen, C.Z. Liu, L.Y. Chang, Y.C. Chen, *Chem. Commun.* (2009) 7515–7517.
- [32] S.Y. Lin, N.T. Chen, S.P. Sun, L.W. Lo, C.S. Yang, *Chem. Commun.* (2008) 4762–4764.
- [33] Y.C. Shiang, C.C. Huang, H.T. Chang, *Chem. Commun.* (2009) 3437–3439.
- [34] J.P. Wilcoxon, B.L. Abrams, *Chem. Soc. Rev.* 35 (2006) 1162–1194.
- [35] R. Archana, S. Sonali, M. Deepthy, R. Prasanth, M. Habeeb, P. Thalappil, N. Shantikumar, K. Manzoor, *Nanotechnol.* 21 (2010) 055103–055114.
- [36] J.L. Cheng, T.Y. Yang, C.H. Lee, S.H. Huang, R.A. Sperling, Z. Marco, J.K. Li, J.L. Shen, H.H. Wang, Y.H. Ieh, W.J. Parak, W.H. Chang, *ACS Nano* 3 (2009) 395–401.
- [37] Y.H. Chan, J.X. Chen, Q.S. Liu, S.E. Wark, D.H. Son, J.D. Batteas, *Anal. Chem.* 82 (2010) 3671–3678.
- [38] Y.L. Liu, K.L. Ai, X.L. Cheng, L.H. Huo, L.H. Lu, *Adv. Funct. Mater.* 20 (2010) 951–956.
- [39] H. Wei, Z.D. Wang, L.M. Yang, S.L. Tian, C.J. Hou, Y. Lu, *Analyst* 135 (2010) 1406–1410.
- [40] F. Wen, Y.H. Dong, L. Feng, S. Wang, S.C. Zhang, X.R. Zhang, *Anal. Chem.* 83 (2011) 1193–1196.
- [41] Y.C. Shiang, C.A. Lin, C.C. Huang, H.T. Chang, *Analyst* 136 (2011) 1177–1182.
- [42] H.Y. Liu, X. Zhang, X.M. Wu, L.P. Jiang, C. Burda, J.J. Zhu, *Chem. Commun.* (2011) 4237–4239.
- [43] K.S. Suslick, *Science* 247 (1990) 1439–1442.
- [44] Z.Q. Yuan, M.H. Peng, Y. He, E.S. Yeung, *Chem. Commun.* 47 (2011) 11981–11983.
- [45] M.F. Mousavi, A. Jabbari, S. Nourvozi, *Talanta* 45 (1998) 1247–1253.
- [46] H. Li, C.J. Meininger, G.Y. Wu, *J. Chromatogr. B* 746 (2000) 199–207.
- [47] P. Kleinbongard, T. Rassaf, A. Dejam, S. Kerber, M. Kelm, *Methods Enzymol.* 359 (2003) 158–168.
- [48] X. Liu, L. Guo, L.X. Cheng, H.X. Ju, *Talanta* 78 (2009) 691–694.
- [49] X.W. Chen, F. Wang, Z.L. Chen, *Anal. Chim. Acta* 623 (2008) 213–220.
- [50] L. Wang, J.G. Chen, H.Q. Chen, C.L. Zhou, B. Ling, J. Fu, *J. Lumin.* 131 (2011) 83–87.
- [51] T. Zhang, H.L. Fan, Q.H. Jin, *Talanta* 81 (2010) 95–99.